

Use of Phosphoimidazolidine-Activated Guanosine To Investigate the Nucleophilicity of Spermine and Spermidine

Anastassia Kanavarioti,* Eldon E. Baird, and Pearish J. Smith

Department of Chemistry and Biochemistry, University of California, Santa Cruz, California 95064

Received October 5, 1994 (Revised Manuscript Received May 15, 1995[®])

Guanosine 5'-phosphate 2-methylimidazolidine (2-MeImpG), a labile phosphoimidazolidine analog of guanosine triphosphate, was used to test the reactivity of the natural polyamines (PAs), spermine (spm) and spermidine (spd). The products are the guanosine 5'-phosphate-polyamine derivatives (PA-pG: spd-pG and spm-pG) which are quite stable in the range $4 < \text{pH} < 11$. Our study is the first of which we are aware that reports on the nucleophilicity of these amines. The main findings are as follows. (i) HPLC analysis of the products indicates the formation of only two of the three possible spd products and only one of the two possible spm products. These results can be explained if only the primary amino groups of the two polyamines are reactive, while the secondary amino groups are rendered unreactive by a steric effect. The reactions of 2-MeImpG and other phosphoimidazolidine derivatives of nucleosides (ImpNs) with primary and secondary monoamines support this interpretation (Kanavarioti et al. *J. Org. Chem.* **1995**, *60*, 632). (ii) The product ratio of the two spd-pG adducts derived from the primary amino groups varies between 2.40 and 0.71 in the range $6.1 \leq \text{pH} \leq 11.9$. Such small variation in the product ratio can only be rationalized by the similar, but not identical, basicity of the two primary amino groups and provides strong support for a previously reported model for polyamine ionization (Onasch et al. *Biophys. Chem.* **1984**, *19*, 245). (iii) On the basis of our kinetic determinations conditions at which the nucleophilicity of these amines is at a minimum and at which other interactions with ImpNs could be tested can be chosen.

Polyamines (PAs) are ubiquitous, found both in eukaryotes (spermidine (spd) and spermine (spm)) and prokaryotes (spd and putrescine) and considered necessary for proper cell function and growth.¹ The mechanism by which PAs promote and regulate growth in the cell is not well-understood. What has been established so far is that PAs which, in neutral aqueous solution are mainly present as polyammonium ion, form complexes with mononucleotides in aqueous solution.² They have a high affinity for DNA and RNA double helices, as would be expected for a positively charged polycation attracted to a negatively charged polyanion, although recent evidence points to interactions between ammonium groups and donor atoms on the bases.^{3,4} Diamines were shown to be effective catalysts in the hydrolysis of single-stranded homoribonucleic acids, and the bifunctional nature of the catalyst was noted.⁵ It was proposed that the amino group promoted the 2'-OH nucleophilic reaction on the phosphorus and the ammonium group assisted the 5'-phosphate leaving group departure.⁵ Although PAs do not seem to catalyze the hydrolysis of the triphosphates of the nucleosides, analogs of PAs do. This was shown by the extensive investigations of Lehn and co-workers with polyammonium macrocycles.^{6,7a} One

macrocycle in particular, [24]N₆O₂, exhibits enhanced activity in catalyzing ATP hydrolysis,^{8,9} pyrophosphate formation,¹⁰ and formate activation.¹¹ Both the hydrolysis and the latter two bond-forming reactions occur by electrostatic stabilization of the substrate within the macrocycle and via formation of a phosphoramidate intermediate, similar in structure with the polyamine derivatives of guanosine studied here.

In order to gain insight into the reactivity of PAs, a suitable electrophile had to be chosen. PAs, as well as other amines, react with phosphoimidazolidine derivatives of nucleosides (ImpNs) and replace the imidazole moiety. ImpNs are used in nonenzymatic, template-directed reactions as monomers^{12,13} in place of the natural triphosphate derivatives of the nucleosides. The present work reports on the nucleophilic reactions of spm and spd with guanosine 5'-phosphate 2-methylimidazolidine (2-MeImpG).

Materials and Methods

Materials. 2-MeImpG (96% pure) was synthesized by a modification¹⁴ of a published procedure.¹⁵ 1-Hexanesulfonic acid (1-HSA), spectroscopic grade trifluoroacetic acid (TFA), and 3,3'-diaminodipropylamine (3,3-spd) were purchased from Aldrich and used without further puri-

* Abstract published in *Advance ACS Abstracts*, July 1, 1995.

(1) (a) Tabor, C. W.; Tabor, H. T. *Annu. Rev. Biochem.* **1976**, *45*, 285. (b) Tabor, C. W.; Tabor, H. T. *Annu. Rev. Biochem.* **1984**, *53*, 749.

(2) Nakai, C.; Glinsmann, W. *Biochemistry* **1977**, *16*, 5636.

(3) Stewart, K. D.; Gray, T. A. *J. Phys. Org. Chem.* **1992**, *5*, 461.

(4) (a) Schmid, N.; Behr, J.-P. *Biochemistry* **1991**, *30*, 4357. (b) Zuber, G.; Sirlin, C.; Behr, J.-P. *J. Am. Chem. Soc.* **1993**, *115*, 4939.

(5) Yoshinari, K.; Yamazaki, K.; Komiyama, M. *J. Am. Chem. Soc.* **1991**, *113*, 5899.

(6) Hosseini, M. W.; Blacker, A. J.; Lehn, J.-M. *J. Am. Chem. Soc.* **1991**, *112*, 3896.

(7) (a) Bencini, A.; Bianchi, A.; Garcia-Espana, E.; Scott, E. C.; Morales, L.; Wang, B.; Deffo, T.; Takusagawa, F.; Mertes, M. P.; Mertes, K. B.; Paoletti, P. *Bioorg. Chem.* **1992**, *20*, 8. (b) Wada, T.; Moriguchi, T.; Sekine, M. *J. Am. Chem. Soc.* **1994**, *116*, 9901.

(8) Hosseini, M. W.; Lehn, J.-M.; Maggiora, L.; Mertes, K. B.; Mertes, M. P. *J. Am. Chem. Soc.* **1987**, *109*, 537.

(9) Hosseini, M. W.; Lehn, J.-M.; Jones, K. C.; Plute, K. E.; Mertes, K. B.; Mertes, M. P. *J. Am. Chem. Soc.* **1989**, *111*, 6330.

(10) Hosseini, M. W.; Lehn, J.-M. *J. Am. Chem. Soc.* **1987**, *109*, 7047.

(11) Jahansou, H.; Jiang, Z.; Himes, R. H.; Mertes, M. P.; Mertes, K. B. *J. Am. Chem. Soc.* **1989**, *111*, 1409.

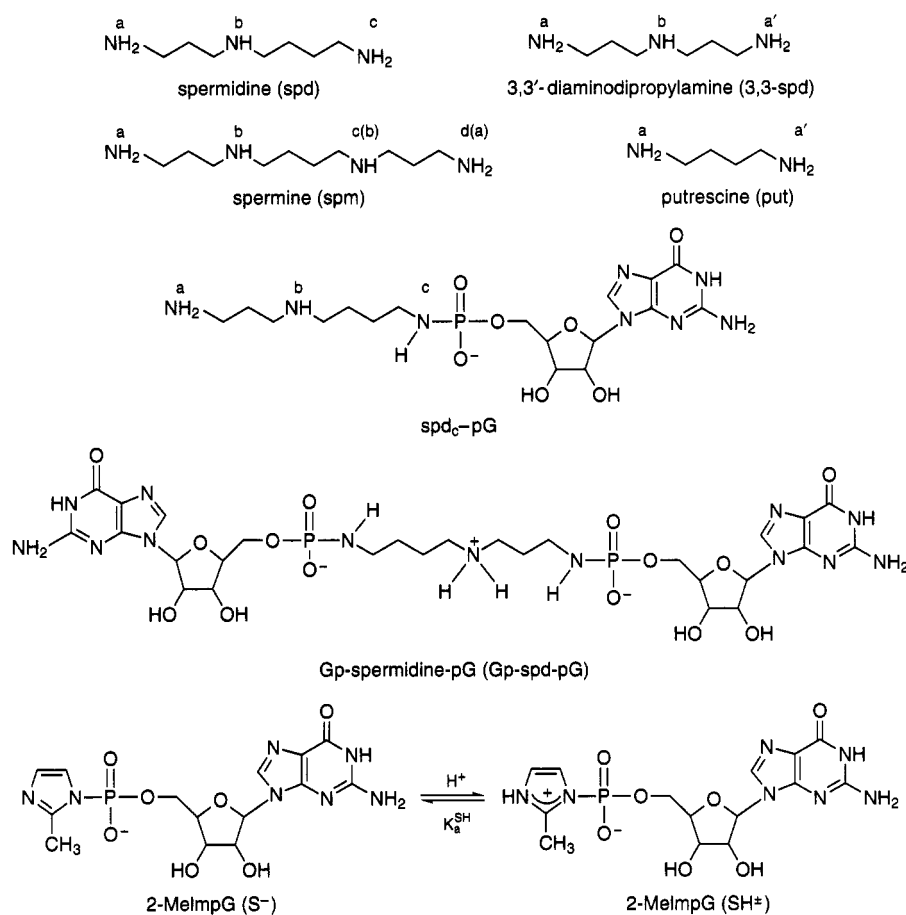
(12) Orgel, L. E. *Nature* **1992**, *358*, 203.

(13) Wu, T.; Orgel, L. E. *J. Am. Chem. Soc.* **1992**, *114*, 7963 and references cited therein.

(14) Kanavarioti, A.; Stronach, M. W.; Ketner, R. J.; Hurley, T. B. *J. Org. Chem.* **1995**, *60*, 632.

(15) Lohrman, R.; Orgel, L. E. *Tetrahedron* **1978**, *34*, 853.

Chart 1



fication. Diguanosine 5'-pyrophosphate (GppG), guanosine 5'-monophosphate (5'GMP), 2-(*N*-morpholino)ethanesulfonic acid (MES), *N*-(2-hydroxyethyl)piperazine-*N'*-(2-ethanesulfonic acid) (HEPES), putrescine, and the HCl salts of spm and spd were purchased from SIGMA. KH₂PO₄, K₂HPO₄, NaCl, and MgCl₂ were purchased from Fisher Scientific. NaOH and HCl solutions were prepared from a "Dilute-it" preparation supplied by Baker. Acetonitrile (HPLC grade) was purchased from Baxter.

Synthesis and Characterization of spm-pG. spm-pG was prepared at pH 9.0 by addition of excess spm in a 0.08 M 2-MelmpG aqueous solution, purified by preparative HPLC on a Waters DeltaPak 25 mm × 100 mm 100 μm C₁₈ column, and isolated as the acetate salt by running a gradient of 10% acetonitrile in a pH 5 acetate buffer. MS (positive-ion FAB in glycerol matrix) was calculated, 548.487, and observed 548.493 (M + 1). The compound is not soluble in DMSO or CHCl₃, and therefore, the ¹H NMR of exchangeable amino protons could not be obtained. ¹H NMR in D₂O integration is consistent with spm:5'GMP = 1:1. ¹³C NMR (D₂O): δ 181.40 (COO⁻ of acetate), 159.31, 154.49, 137.83, 116.63, 87.53, 84.37, 84.26, 74.33, 70.95, 64.30, 64.25 (guanosine moiety), 47.50, 47.21, 45.94, 45.04, 38.49, 37.07, 27.93, 27.86, 24.29, 23.53, 23.29 (spm moiety and CH₃ of acetate). ³¹P NMR: δ 9.278 with external reference 85% H₃PO₄. ¹H and ¹³C NMR spectra were taken on a GE QE 300 instrument, ³¹P spectra on a GE GN 300 NMR spectrometer. The above synthesis that led to the isolation of spm-pG let us also isolate small amounts of the disubstituted derivative of spermine, Gp-spm-pG (structure not shown but similar to Gp-spd-pG which is shown). This compound was characterized by ¹H NMR to have a ratio of

spm:5'GMP of 1:2 by integration of the protons. The symmetry of the molecule was shown by COSY ¹H NMR.

Analysis by High-Performance Liquid Chromatography (HPLC). Samples and solvents were prepared in 18 MΩ-cm HPLC grade water obtained from a Millipore water purifier. HPLC solvents, buffers, ion-pairing agents, and electrolytes were filtered through a 0.45 μm HA Millipore filter or through a Nylon 66 membrane from Alltech Associates under reduced pressure. All HPLC solvents were purged with helium prior to use. Analysis was performed with a 1090 Hewlett-Packard LC system using an ODS Hypersil C₁₈ column (5 μm, 200 mm × 4.6 mm) supplied by Hewlett-Packard. The reaction mixtures were monitored at 254 nm where the guanine moiety absorbs, but not the amine or the imidazole. We developed two systems: 1-HSA and TFA. Most kinetics were performed with the TFA, but product analysis was performed with the 1-HSA system because the latter resolved the two isomeric spd-pG products the best. TFA System: solvent A, 0.05M KH₂PO₄, 0.2% (wt/v) TFA; Solvent B, 0.05 M KH₂PO₄, 30% (v/v) acetonitrile, 0.2% (wt/v) TFA; pH, 2.1–2.4; gradient elution, 0–17% solvent B in 8 min, isocratic 17% B for 4 min, 17 to 30% B in 4 min; retention times, 5'GMP *t*_R 4.9 min, GppG *t*_R 7.5 min, 2-MelmpG *t*_R 8.9 min, putrescine-pG *t*_R 9.1 min, (3,3)-spd-pG *t*_R 9.5 min, spd-pG *t*_R 10.1 min, spm-pG *t*_R 10.9 min; Gp-(3,3)-spd-pG *t*_R 11.6 min, Gp-spd-pG *t*_R 12.1 min, Gp-spm-pG *t*_R 13.3 min. 1-HSA System: solvent A, 0.05 M KH₂PO₄, 2 × 10⁻⁴ M 1-HSA; solvent B, 0.05 M KH₂PO₄, 2 × 10⁻⁴ M 1-HSA, 30% (v/v) acetonitrile; pH, 2.1–2.4; gradient elution, 0 to 20% B in 13 min, isocratic 20% B for 7 min; retention times, 5'GMP *t*_R 8.7 min,

GppG t_R 12.4 min, 2-MeImpG t_R 12.4 min, (3,3)-spd-pG t_R 12.7 min, spd-pG_a t_R 14.1 min, spd-pG_c t_R 14.9 min, spm-pG t_R 15.9 min, Gp-(3,3)-spd-pG t_R 14.7 min, Gp-spd-pG t_R 16.1 min, Gp-spm-pG t_R 16.6 min.

Solutions and Kinetics. Reactions were run at 37 °C ± 0.3 °C, which was maintained using the thermostated autosampler of the HP 1090 liquid chromatograph. The concentration of 2-MeImpG was typically 5×10^{-4} M. The concentration of polyamine ranged from 0.003 to 0.05 M, so that pseudo-first order conditions were maintained. An ionic strength of 1 M was maintained with NaCl as the compensating electrolyte. The contribution of the polyamine to the ionic strength was estimated by viewing protonated amino groups as point charges. For example, a 1 mM spd·3HCl solution would be calculated to have an ionic strength of 3 mM. Reactions were monitored for at least one half-life, and excellent pseudo-first-order kinetics were obtained. Values of k_{obsd} , with an estimated error of less than ±5%, were obtained from a plot of $\ln(\% \text{ area of 2-MeImpG})$ as a function of time. Because all monomeric guanosine derivatives have identical, within experimental error, extinction coefficients, the total area was calculated by adding the areas of all the peaks with a guanosine UV-vis spectrum. All pH measurements were made using a MI 410 microelectrode supplied by Microelectrodes Inc. at 23 °C. The pH was maintained within ±0.02 units by buffering the system with the polyamine or with an external buffer (HEPES or MES) when necessary.

Plots of k_{obsd} vs total amine concentration were constructed using six separate samples at different amine concentrations. S_k values were determined by least squares analysis directly from the slope of a plot of k_{obsd} vs total amine concentration. For pH < 8.6, the data were fit by straight lines; for pH ≥ 8.6, the data showed slight downward curvature and were fit with a second-order fit, and S_k was set equal to the initial slope. The curvature was attributed to an enhanced association between protonated and deprotonated amine species that became progressively more important as the pH increased and the amount of deprotonated amine was comparable to that of the protonated amine. It is reasonable to assume that this association resulted in somewhat decreased reactivity as manifested by the downward curvature in the buffer plots. Not only was the second-order fit a better match for the experimental data, but it also provided values for the intercepts which were in much better agreement with the predicted values, I (from ref 16a, $I = [H^+](k_{\text{SH}}^w + k_{\text{SH}}^{\text{OH}}[\text{OH}^-]) / (K_a^{\text{SH}} + [H^+])$), than the intercepts obtained via a straight line correlation. Values of I are listed in Table 1. Product ratios, defined as [spd-pG]/[5'GMP] or [spm-pG]/[5'GMP], were obtained with good accuracy and reported for experiments at pH < 8.8 (Tables S2 and S3 in the supporting information).¹⁷ Product ratios were obtained from $(\text{area}(\text{PA-pG}) - \text{area}(\text{PA-pG})_0) / (\text{area}(5'\text{GMP}) - \text{area}(5'\text{GMP})_0)$ where $\text{area}(\text{PA-pG})_0$ and $\text{area}(5'\text{GMP})_0$ are the observed areas in the first analysis of the sample. These corrections are necessary because 5'GMP is a substrate impurity and because both the amine substitution product and 5'GMP are produced before the temperature of the samples equilibrates to 37 °C.

Table 1. Kinetic Parameters determined from the Reaction of 2-MeImpG with spd and spm at 37 °C and $\mu = 1.0$ M with NaCl

| amine | pH | $10^9 \times [H^+],$ M | S_k, M^{-1} h^{-1a} | $10^3 \times I,$ h^{-1b} | $S_p,$ M^{-1c} | $S_k/I,$ M^{-1} |
|-------|------|---------------------------|----------------------------|-------------------------------|---------------------|----------------------|
| spd | 7.50 | 31.6 | 2.11 | 9.48 | 205 | 223 |
| | 7.99 | 10.2 | 2.49 | 3.93 | 507 | 634 |
| | 8.13 | 7.41 | 2.38 | 3.00 | 703 | 793 |
| | 8.19 | 6.46 | 2.44 | 2.67 | 928 | 914 |
| | 8.63 | 2.34 | 2.60 | 1.17 | 1372 | 2220 |
| | 9.02 | 0.955 | 2.15 | 0.63 | — | 3413 |
| | 9.32 | 0.479 | 2.02 | 0.44 | — | 4590 |
| | 9.52 | 0.302 | 1.78 | 0.37 | — | 4811 |
| | 9.72 | 0.191 | 1.49 | 0.32 | — | 4656 |
| | spm | 6.16 | 69.2 | 0.52 | 29.7 | 15.6 |
| 6.92 | | 12.0 | 1.86 | 20.0 | 84.7 | 93.0 |
| 7.70 | | 20.0 | 2.89 | 6.74 | 321 | 429 |
| 8.12 | | 7.59 | 3.16 | 3.06 | 924 | 1033 |
| 8.59 | | 2.57 | 3.19 | 1.26 | 1554 | 2532 |
| 8.83 | | 1.48 | 2.77 | 0.84 | 2371 | 3300 |
| 9.27 | | 0.537 | 2.34 | 0.46 | — | 5087 |
| 9.81 | | 0.155 | 1.52 | 0.31 | — | 4903 |
| 10.03 | | 0.093 | 1.16 | 0.28 | — | 4143 |

^a S_k values were obtained from the slope of the plots of k_{obsd} as a function of total amine concentration. ^b I values were calculated as described in the Materials and Methods. ^c S_p values were obtained from the slope of the plot of the product ratio, [PA-pG]/[5'GMP], determined by HPLC as a function of total amine concentration.

Macroscopic Acidity Constants of spm and spd. pK values were determined potentiometrically at room temperature (23 ± 1 °C), and the 1.0 M ionic strength was maintained with NaCl. For spd, the constants are 8.88, 10.15, and 11.06 for pK₁, pK₂, and pK₃, respectively; for spm, the constants are 8.60, 9.33, 10.45, and 11.23 for pK₁, pK₂, pK₃, and pK₄, respectively. These values are accurate to ±0.05. They were obtained by pseudo-titration; i.e., a specific amount of strong base, NaOH, was added to a known amount of fully protonated amine (spd·3HCl or spm·4HCl), and the pH was measured (Table S1 in the supporting information).¹⁷ Evaluation of pKs was based on eq 1 which describes the charge balance for an acid AH⁺ titrated with a strong base, such as NaOH.¹⁸ In eq 1, [AH] and [NaOH] stand for the molar concentrations of weak acid and added base; [H⁺] is the hydrogen ion activity and [OH⁻] the hydroxide ion activity, calculated from pH and K_w . X represents the degree of ionization, so that [AH] X is equal to the equivalents of deprotonated acid. For spd, X is given by eq 2, and for spm, X is given by eq 3.

$$[\text{AH}]X = [\text{NaOH}] + [\text{H}^+] - [\text{OH}^-] \quad (1)$$

$$X(\text{spd}) = \frac{[\text{H}_2\text{spd}^{2+}] + 2[\text{Hspd}^+] + 3[\text{spd}^0]}{[\text{spd}]_{\text{tot}}} \quad (2)$$

$$X(\text{spm}) = \frac{[\text{H}_3\text{spm}^{3+}] + 2[\text{H}_2\text{spm}^{2+}] + 3[\text{Hspm}^{1+}] + 4[\text{spm}^0]}{[\text{spm}]_{\text{tot}}} \quad (3)$$

In eqs 2 and 3, the concentration of each species can be expressed as a function of the pKs and the pH based on eqs 4–7 for eq 2 and eqs 9–13 for eq 3. X is easily calculated from the pseudo-titration data. A set of pKs was found by iterative fitting, using either Microsoft

(16) (a) Kanavarioti, A.; Rosenbach, M. T. *J. Org. Chem.* **1991**, *56*, 1513. (b) Kanavarioti, A.; Rosenbach, M. T.; Hurley, T. B. *Origins Life* **1992**, *21*, 199.

(17) See paragraph concerning the supporting information at the end of this paper.

(18) Hamann, S. D. *Aust. J. Chem.* **1970**, *23*, 1749.

Excel or Eureka the Solver, so that all the experimentally determined X values are matched to a deviation of less than 2% with spm and less than 1% with spd. The good quality of the determined pK_a values is demonstrated by the symmetry in a distribution profile of the various spm species over the range $6.5 \leq \text{pH} \leq 13$ illustrated in Figure S1 in the supporting information.¹⁷

$$[\text{H}_3\text{spd}^{3+}]/[\text{spd}]_{\text{tot}} = [\text{H}^+]/K_1 F_{\text{spd}} \quad (4)$$

$$[\text{H}_2\text{spd}^{2+}]/[\text{spd}]_{\text{tot}} = 1/F_{\text{spd}} \quad (5)$$

$$[\text{Hspd}^+]/[\text{spd}]_{\text{tot}} = K_2/[\text{H}^+] F_{\text{spd}} \quad (6)$$

$$[\text{spd}^0]/[\text{spd}]_{\text{tot}} = K_2 K_3/[\text{H}^+]^2 F_{\text{spd}} \quad (7)$$

where

$$F_{\text{spd}} = \frac{[\text{H}^+]}{K_1} + 1 + \frac{K_2}{[\text{H}^+]} + \frac{K_2 K_3}{[\text{H}^+]^2} \quad (8)$$

$$[\text{H}_4\text{spm}^{4+}]/[\text{spm}]_{\text{tot}} = [\text{H}^+]/K_1 F_{\text{spm}} \quad (9)$$

$$[\text{H}_3\text{spm}^{3+}]/[\text{spm}]_{\text{tot}} = 1/F_{\text{spm}} \quad (10)$$

$$[\text{H}_2\text{spm}^{2+}]/[\text{spm}]_{\text{tot}} = K_2/[\text{H}^+] F_{\text{spm}} \quad (11)$$

$$[\text{Hspm}^+]/[\text{spm}]_{\text{tot}} = K_2 K_3/[\text{H}^+]^2 F_{\text{spm}} \quad (12)$$

$$[\text{spm}^0]/[\text{spm}]_{\text{tot}} = K_2 K_3 K_4/[\text{H}^+]^3 F_{\text{spm}} \quad (13)$$

where

$$F_{\text{spm}} = \frac{[\text{H}^+]}{K_1} + 1 + \frac{K_2}{[\text{H}^+]} + \frac{K_2 K_3}{[\text{H}^+]^2} + \frac{K_2 K_3 K_4}{[\text{H}^+]^3} \quad (14)$$

Results

Characterization of spm-pG and Gp-spm-pG by NMR Techniques. The reaction of spm with 2-MeImpG was run in milligram quantities, and spm-pG and Gp-spm-pG were isolated (see the Materials and Methods). ¹H, ¹³C, and ³¹P NMR for spm-pG were consistent with the presence of a pure material with a composition spm:5'GMP = 1:1; ¹H NMR of Gp-spm-pG (COSY) indicates a symmetrical derivative with spm:5'GMP = 1:2. Comparison between the ¹³C NMR of spermine and that of spm-pG indicates that the symmetry of the spm molecule is lost and that the spm carbons that were equivalent in spm are no longer equivalent in spm-pG. However, determination of the P-N site (primary vs secondary amino group) on the basis of the NMR data is not straightforward for the following reason: All carbons, not only the one(s) closer to the substituted nitrogen, exhibit small chemical shifts as compared to the ones observed with spm. This is not uncommon. Indeed, substitution of the N-H bond of an amino group by the P-N bond of a phosphoramidate produces comparable chemical shifts in the ¹³C NMR up to seven bonds away from the point of substitution (see ¹³C NMR of *O,O*-diphenylphosphoramidate of [21]aneN₇ in ref 7a; see also ref 7b).

How Many PA-pG Derivatives? Despite a great deal of effort in developing appropriate chromatography, we observed only two spd-pG products and one spm-pG (NMR of spm-pG also indicates pure material, see above)

product instead of the expected three and two, respectively. In order to show that we did not miss any products, the following control experiments were performed. (i) In the reaction with putrescine (not reported), we observed only one peak, as expected. This experiment dispelled the possibility that our chromatography does not resolve the amine derivatives but leads to artificially split peaks. (ii) We tested reaction mixtures of 3,3-spd which is a symmetrical amine with a structure very similar to spd. This amine is expected to give two products, but we only observed one. (iii) When [2-Me-ImpG] \approx [PA], there is evidence of only one additional product, the disubstituted amine (Gp-spm-pG and Gp-spd-pG). If secondary and primary amino groups were of comparable reactivity, then one would expect, in addition to the three monosubstituted derivatives, the formation of one tri- and three disubstituted spd derivatives. Similarly, with spm, in addition to the two monosubstituted derivatives, up to one tetra-, two tri-, and four disubstituted derivatives could be formed. It is very likely that even the simplest chromatography system would resolve products that vary by a whole 5'GMP moiety, e.g. the di- from the trisubstituted, and unlikely that all these derivatives were present and eluted as a single peak.

The above experiments taken together strongly suggest that it is only the primary amino groups that are reactive. In order to dispel any doubt, we investigated the nucleophilicity of a series of primary and secondary alicyclic and aliphatic amines with 2-MeImpG and other selected ImpNs.¹⁴ We found that the successive addition of ethyl groups to the same nitrogen creates substantial steric hindrance and leads to an at least 100-fold reactivity difference between diethylamine and a primary amine of similar basicity. These results corroborate the observation that with PAs it is only the primary amino groups that are reactive and that the secondary ones are rendered virtually unreactive due to a strong steric effect.

Experiments Performed with [2-MeImpG] \approx [PA].

In this type of experiment, relatively large amounts of the disubstituted PA are formed. In order to estimate the pK_a of the substituted amino group in PA-pG and Gp-PA-pG products, pH jump experiments were performed. Samples containing either 0.001 M 2-MeImpG or 0.05 M 2-MeImpG and 0.05 M polyamine were prepared at pH 7 and incubated at 0, 7, and 37 °C until most of the substrate had reacted (about 450, 110, and 90 h, respectively). Then the pH was dropped by addition of HCl to either pH 5 or 2, and the sample was allowed to hydrolyze at 37 °C. It was found that both, Gp-PA-pG and PA-pG, are quite stable at pH 5, but hydrolyze rapidly at pH 2. The stability of these materials at pH 5 indicates that their pK_a is less than 5, perhaps closer to 3. As expected, the disubstituted product hydrolyzes with a rate approximately twice that of the monosubstituted product which, in turn, hydrolyzes about 6 times faster than 2-MeImpG at pH 2. It should be noted that experiments with another nucleotide, cytidine 5'-monophosphate 2-methylimidazole (not reported here), also indicate the formation of two types of amine substitution products, most likely the mono- and disubstituted derivatives of spd and spm, in perfect agreement with the observations made with 2-MeImpG. The possibility that the mono- or disubstituted polyamine derivatives of the nucleotides could be used as activated substrates for nucleotide oligomerizations is under further investigation in our lab, although their stability at neutral pH renders

them less promising than the phosphoimidazolides. In contrast to the facile reaction of PAs with 2-MeImpG, all our attempts to detect aminolysis of guanosine 5'-triphosphate with spm or spd under similar conditions failed.

Kinetics and Product Distribution of the Reaction of 2-MeImpG with spd and spm. Experiments were performed at 37 ± 0.3 °C in aqueous solution in the range $6.1 \leq \text{pH} \leq 11.9$ with spd, and $6.2 \leq \text{pH} \leq 11.0$ with spm. Samples were analyzed by HPLC as described in the Materials and Methods. Values of k_{obsd} as a function of total amine concentration are listed in Table S2 for spd and Table S3 for spm in the supporting information.¹⁷ In these tables, the corresponding product ratios are also included. Product ratios as a function of total amine concentration provided straight lines with zero intercepts and slopes identified as S_p . These slopes (S_p) as well as the slopes of the buffer plots (k_{obsd} as a function of total amine concentration), identified as S_k , are summarized in Table 1. How we obtained the slopes is described in detail in the Materials and Methods. Intercepts of the buffer plots (not reported, see the Materials and Methods) were in very good agreement with the calculated values, I , and are reported in Table 1. Because of the long extrapolation to the intercept, the calculated values were considered more accurate than the observed intercepts. Reaction rates were seen to increase with amine concentration but decrease with increasing pH. The amine derivative is favored over the hydrolysis product with increasing pH and amine concentration. These observations are consistent with the mechanism proposed below (eq 15) which is similar to the one for reactions with other nucleophiles.¹⁶

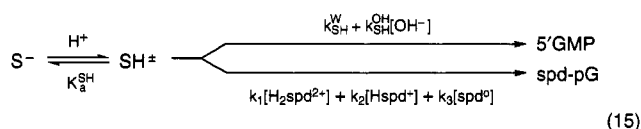
The Mechanism of Nucleophilic Substitution at

(19) (a) Kanavarioti, A. *Origins Life* **1986**, *17*, 85. (b) Kanavarioti, A.; Bernasconi, C. F.; Doodokyan, L. D.; Alberas, D. J. *J. Am. Chem. Soc.* **1989**, *111*, 7247.

(20) Ruzicka, F. J.; Frey, P. A. *Bioorg. Chem.* **1993**, *21*, 238.

(21) A referee has suggested that the $k_{\text{SH}}^{\text{OH}}[\text{OH}^-]$ term be dropped because, according to Ruzicka and Frey,²⁰ "this process has been proven to make no significant contribution to the mechanism of ImpU and 2-MeImpU hydrolysis." There are two erroneous assumptions underlying this suggestion. The first one is that, even if it could be proven that the $k_{\text{SH}}^{\text{OH}}[\text{OH}^-]$ term which corresponds to the reaction of the zwitterionic form of 2-MeImpG (SH^\pm) is insignificant, the term could not just be "dropped." The rate law would then require that it be replaced by a term for the kinetically indistinguishable reaction of the anionic form of 2-MeImpG (S^-) with water. However, Kanavarioti et al.^{19b} have shown that the reaction of SH^\pm with OH^- probably contributes more to the overall rate than the reaction of $\text{S}^- + \text{H}_2\text{O}$. The second erroneous assumption goes back to the claim that the $\text{SH}^\pm + \text{OH}^-$ pathway is negligible compared to the $\text{S}^- + \text{H}_2\text{O}$ pathway. However, this "proof" is based on a misinterpretation. Specifically, the $\text{SH}^\pm + \text{OH}^-$ pathway is thought to be unimportant because the hydrolysis of N-MeImpU, which can be regarded as a model for the zwitterionic form of ImpU and was assumed to have the same reactivity, "should exhibit a marked increase in rate with increasing pH throughout the pH range", whereas in fact, "the hydroxide ion dependence does not appear at pH values less than 10." However, the pH at which the hydroxide ion dependence in the hydrolysis of N-MeImpU starts to become significant is only one of several relevant factors; what determines whether or not the $\text{SH}^\pm + \text{OH}^-$ pathway contributes significantly to the pH-independent hydrolysis of ImpU is the relative magnitude of $k_{\text{SH}}^{\text{OH}}(K_w/K_a^{\text{SH}})$ vs k_{S}^w . On the basis of $\text{p}K_a^{\text{SH}} = 5.68$ for ImpU and $K_w = 2 \times 10^{-14} \text{ M}^{-2}$ at 1.0 M NaCl³⁰ and assuming that $k_{\text{SH}}^{\text{OH}}$ is the same as the rate constant for reaction of N-MeImpU with OH^- ($6.17 \times 10^3 \text{ M}^{-1} \text{ h}^{-1}$), one obtains $k_{\text{SH}}^{\text{OH}}(K_w/K_a^{\text{SH}}) = 5.91 \times 10^{-5} \text{ h}^{-1}$. This compares with $2.1 \times 10^{-4} \text{ h}^{-1}$ for what is not just k_{S}^w but must be the sum $k_{\text{SH}}^{\text{OH}}(K_w/K_a^{\text{SH}}) + k_{\text{S}}^w$. This shows that the $\text{SH}^\pm + \text{OH}^-$ pathway contributes 28% to the overall rate. For 2-MeImpG, $\text{p}K_a^{\text{SH}} = 7.09$ is considerably higher than for ImpU (5.68); assuming that the $k_{\text{SH}}^w/k_{\text{SH}}^{\text{OH}}$ ratio is not significantly different for 2-MeImpG, the higher $\text{p}K_a^{\text{SH}}$ should result in a considerably larger $k_{\text{SH}}^{\text{OH}}(K_w/K_a^{\text{SH}})$ term, making the $\text{SH}^\pm + \text{OH}^-$ pathway dominant in the 2-MeImpG system, as suggested earlier.^{19b}

the P–N Bond. The hydrolysis of 2-MeImpG has been studied in detail in the range $2 \leq \text{pH} \leq 13$,^{19ab} and it was concluded that, up to pH 10.5, P–N bond cleavage occurs via water and/or OH^- attack on the species which is protonated at the imidazole moiety, SH^\pm (see structures, $\text{p}K_a$ 7.09 for 2-MeImpG). Reaction of the deprotonated substrate, S^- , with PA is negligible under our conditions at $\text{pH} < 10.5$.¹⁴ A mechanism which excludes the OH^- pathway for this pH range has been proposed for the hydrolysis of the uridine phosphoimidazolides,²⁰ but this mechanism seems incomplete even for those substrates for which it was postulated.²¹ In any case, even if the different interpretation²⁰ were correct, it would not affect the numerical calculations of this study. The mechanism proposed for the reaction of 2-MeImpG with spd is given by eq 15. In eq 15, $k_{\text{SH}}^w = 3.32 \times 10^{-2} \text{ h}^{-1}$ and $k_{\text{SH}}^{\text{OH}} = 9.52 \times 10^2 \text{ M}^{-1} \text{ h}^{-1}$,^{16a} k_1 , k_2 , and k_3 are the rate constants for the nucleophilic displacement of 2-methylimidazole by the monodeprotonated, dideprotonated, and fully deprotonated spd species, respectively.



Determination of Macroscopic Rate Constants for spd. Based on eq 15, the observed pseudo-first-order rate constant, k_{obsd} , for the disappearance of 2-MeImpG is given by eq 16

$$k_{\text{obsd}} = \frac{[\text{H}^+]}{K_a^{\text{SH}} + [\text{H}^+]} (k_{\text{SH}}^w + k_{\text{SH}}^{\text{OH}}[\text{OH}^-] + k_1[\text{H}_2\text{spd}^{2+}] + k_2[\text{Hspd}^+] + k_3[\text{spd}^0]) \quad (16)$$

S_k , the slope of a plot of k_{obsd} as a function of total spd concentration, is given by eq 17 after substituting the concentrations of the various spd species using eqs 5–7.

$$S_k = \frac{[\text{H}^+]}{K_a^{\text{SH}} + [\text{H}^+]} \left(\frac{k_1}{F_{\text{spd}}} + k_2 \frac{K_2}{[\text{H}^+]F_{\text{spd}}} + k_3 \frac{K_2 K_3}{[\text{H}^+]^2 F_{\text{spd}}} \right) \quad (17)$$

There are two obvious ways to rearrange eq 17: to eq 18 or to eq 19. By plotting the left-hand term of eq 18 vs $1/[\text{H}^+]$, the rate constants k_1 , k_2 , and k_3 can be deduced from the fit of the curve to the data and the known acidity constants (Figure 1). The absence of curvature in Figure

$$\frac{[\text{H}^+] + K_a^{\text{SH}}}{[\text{H}^+]} S_k F_{\text{spd}} = k_1 + \frac{k_2 K_2}{[\text{H}^+]} + \frac{k_3 K_2 K_3}{[\text{H}^+]^2} \quad (18)$$

$$S_k F_{\text{spd}} ([\text{H}^+] + K_a^{\text{SH}}) = k_1 [\text{H}^+] + k_2 K_2 + k_3 \frac{K_2 K_3}{[\text{H}^+]} \quad (19)$$

1 indicates that k_3 does not contribute significantly in the pH range studied. It is actually $[\text{spd}^0]$ which is negligible; using eq 9, we calculate $[\text{spd}^0]/[\text{spd}]_{\text{tot}} = 0.01$ at pH 9.72 which is the highest pH used in the kinetic runs. Therefore, k_3 cannot be obtained from our data. Analysis of Figure 1 provides an intercept $k_1 = 181 \text{ M}^{-1} \text{ h}^{-1}$ and a slope of 1.54×10^{-7} which gives $k_2 = 2175 \text{ M}^{-1} \text{ h}^{-1}$. The analysis of the data using eq 19 also shows a linear fit of the left-hand term with $[\text{H}^+]$ and provides

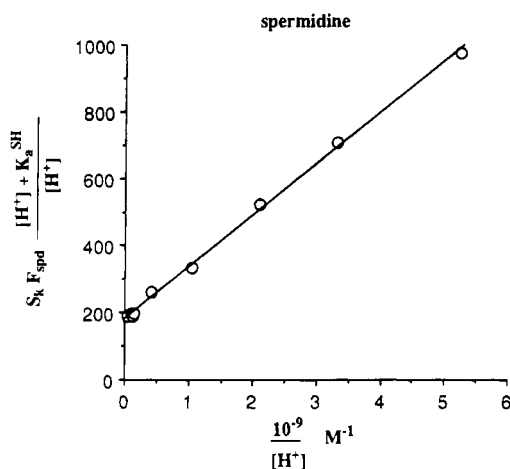


Figure 1. Analysis of the kinetic data with spermidine according to eq 18 (see the text). Straight line drawn through the data points.

Table 2. Product Distribution Analysis of the Two spd-pG Isomers

| pH | [spd] _{tot} , M | [spd _a -pG]/[spd _c -pG] |
|-------|--------------------------|---|
| 11.87 | 0.05 | 0.71 |
| 11.35 | 0.05 | 0.76 |
| 11+ | 0.05 | 0.76 ± 0.03 |
| 10.79 | 0.05 | 0.76 |
| 9.9 | 0.01 | 1.10 |
| | 0.03 | 1.10 ± 0.04 |
| | 0.05 | 1.00 ± 0.01 |
| 8.8 | 0.05 | 1.69 ± 0.06 |
| 7.9 | 0.05 | 2.17 ± 0.09 |
| 7.0 | 0.05 | 2.50 ± 0.14 |
| 6.1 | 0.05 | 2.40 ± 0.11 |

Table 3. Macroscopic and Microscopic Acidity and Rate Constants for the Reaction of Spermidine with 2-MelmpG at 37 °C and μ = 1.0 M

| rate constants, M ⁻¹ h ⁻¹ ^a | | pK ^b | | p/q ^c | pK + log p/q ^c | log k/q ^c |
|--|-----------|------------------|---------------|------------------|---------------------------|----------------------|
| k ₁ | 182 ± 4 | K ₁ | 8.88 (8.51) | | | |
| k ₂ | 2100 ± 80 | K ₂ | 10.15 (10.02) | | | |
| k ₃ | — | K ₃ | 11.06 (11.02) | | | |
| | | K _{acb} | 9.13 (8.76) | | | |
| k _a ²⁺ | 353 | K _{cba} | 9.34 (8.97) | 3/1 | 9.82 | 2.55 |
| k _c ²⁺ | 686 | K _{abc} | 9.94 (9.57) | 3/1 | 10.42 | 2.84 |
| k _a ⁺ | 1814 | K _{ca} | 10.31 (10.18) | 3/1 | 10.79 | 3.26 |
| k _{ba} ⁺ | 2240 | K _{ac} | 10.50 (10.37) | 3/1 | 10.98 | 3.35 |
| k _{bc} ⁺ | 1504 | K _{bc} | 10.14 (10.01) | 3/1 | 10.62 | 3.18 |
| k _{ac} ⁻ | 775 | K _{ba} | 9.54 (9.41) | 3/1 | 10.02 | 2.89 |
| k _{ca} ⁻ | | K _{ab} | 9.69 (9.56) | | | |
| | | K _{cb} | 10.11 (9.98) | | | |
| | | K _a | 10.46 (10.42) | | | |
| | | K _b | 10.62 (10.58) | | | |
| | | K _c | 10.65 (10.61) | | | |

^a Macroscopic, *k*, and microscopic, *k*, rate constants determined as described in the text. The subscripts of the microscopic rate constants indicate the basic nitrogens, and the last letter indicates the nucleophilic one. ^b Macroscopic acidity constants, *K*, in this work were determined by pseudo-titration (see the Materials and Methods). For the notation for microscopic acidity constants, *K*, see Figure 4. Values in parentheses were determined by NMR.^{22a} Microscopic acidity constants for this work were determined by extrapolation of the corresponding values from ref 22a (see the text). ^c Statistical corrections: *p* = number of ionizable protons, *q* = number of basic sites.

values of *k*₁ = 183 M⁻¹ h⁻¹ and *k*₂ = 2020 M⁻¹ h⁻¹. The average values *k*₁ = 182 M⁻¹ h⁻¹ and *k*₂ = 2100 M⁻¹ h⁻¹ are reported in Table 3.

Determination of Macroscopic Rate Constants with spm. A similar analysis can be applied toward extracting macroscopic rate constants from the spm data.

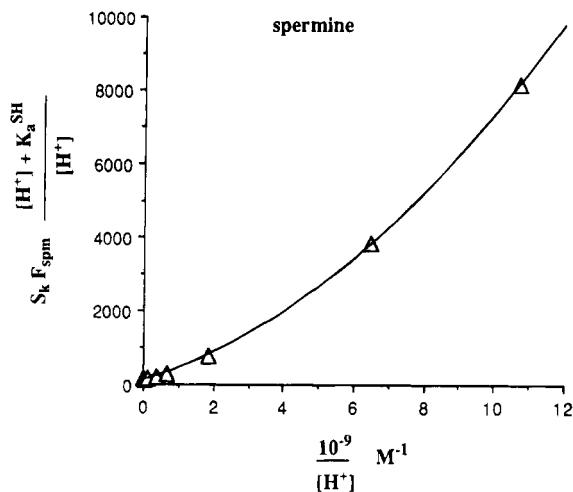
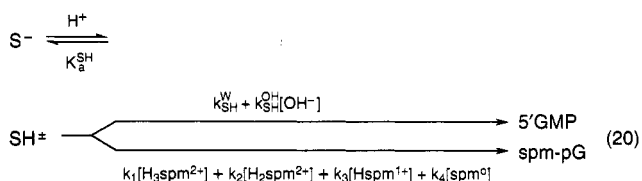


Figure 2. Analysis of the kinetic data with spermine according to eq 23 (see the text). Data correlate with a second-order fit.

Equation 20 represents the reaction of spm with 2-Me-ImpG; *k*₁, *k*₂, *k*₃, and *k*₄ are rate constants for the nucleophilic displacement of 2-methylimidazole by the mono-, di-, and trideprotonated and fully deprotonated spm species, respectively. Equation 21 is the rate law where *k*_h = *k*_w^{SH} + *k*_{OH}^{SH}[OH⁻]. The concentration of each spm species can be calculated from eqs 10–13. The slope,



$$k_{obsd} = \frac{[H^+]}{K_a^{SH} + [H^+]} (k_h + k_1[H_3spm^{2+}] + k_2[H_2spm^{2+}] + k_3[Hspm^{1+}] + k_4[spm^0]) \quad (21)$$

*S*_k of a plot of *k*_{obsd} as a function of total [spm] is given by eq 22, and the rate constants can be obtained by graphing the data as dictated by eq 23 or 24. Figure 2 illustrates the excellent fit obtained using expression 23 for the range 6.92 ≤ pH ≤ 10.03.

$$S_k = \frac{[H^+]}{K_a^{SH} + [H^+]} \left(k_1 \frac{1}{F_{spm}} + k_2 \frac{K_2}{[H^+] F_{spm}} + k_3 \frac{K_2 K_3}{[H^+]^2 F_{spm}} + k_4 \frac{K_2 K_3 K_4}{[H^+]^3 F_{spm}} \right) \quad (22)$$

$$S_k F_{spm} \frac{K_a^{SH} + [H^+]}{[H^+]} = k_1 + k_2 \frac{K_2}{[H^+]} + k_3 \frac{K_2 K_3}{[H^+]^2} + k_4 \frac{K_2 K_3 K_4}{[H^+]^3} \quad (23)$$

$$S_k F_{spm} (K_a^{SH} + [H^+]) = k_1 [H^+] + k_2 K_2 + k_3 \frac{K_2 K_3}{[H^+]} + k_4 \frac{K_2 K_3 K_4}{[H^+]^2} \quad (24)$$

The spm data show a curvilinear dependence on 1/[H⁺]. From eq 12, we calculate that [spm⁺]/[spm]_{tot} = 0.027 at

Table 4. Macroscopic and Microscopic Acidity and Rate Constants for the Reaction of Spermine with 2-MelmpG at 37 °C and $\mu = 1.0$ M

| rate constants, $M^{-1} h^{-1a}$ | | pK^b | | p/q^c | $pK^+ \log p/q^c$ | $\log k/q^c$ |
|-------------------------------------|----------------|-----------------------|--------------------------|---------|-------------------|--------------|
| k_1 | 150 ± 30 | K_1 | 8.60 (7.98, 7.95) | | | |
| k_2 | 640 ± 150 | K_2 | 9.33 (8.94, 8.82) | | | |
| k_3 | 2550 ± 500 | K_3 | 10.45 (10.10, 10.05) | | | |
| k_4 | — | K_4 | 11.23 (10.86, 10.86) | | | |
| k_a^{3+} | 1537 | $K_{abdc} = K_{acdb}$ | 9.00 (8.38) | 6/1 | 10.39 | 3.19 |
| | | $K_{abcd} = K_{bcda}$ | 9.61 (8.99) | | | |
| | | $K_{abc} = K_{cdb}$ | 9.95 (9.56) | | | |
| | | $K_{acb} = K_{bdc}$ | 8.82 (8.43) | | | |
| k_{ba}^{2+} | 4320 | $K_{cda} = K_{abd}$ | 10.56 (10.17) | 3/1 | 11.04 | 3.64 |
| k_{ad}^{2+} | 1684 | $K_{bca} = K_{bcd}$ | 9.38 (8.99) ^d | 3/2 | 9.56 | 2.93 |
| k_{ca}^{2+} | 1239 | $K_{acd} = K_{bda}$ | 9.43 (9.04) ^d | 3/1 | 9.91 | 3.09 |
| | | $K_{adb} = K_{adc}$ | 9.45 (9.06) ^d | | | |
| k_{abd}^+ | 1067 | $K_{ba} = K_{cd}$ | 9.39 (9.04) | 3/1 | 9.87 | 3.03 |
| k_{dba}^+ | 3724 | $K_{ca} = K_{bd}$ | 10.52 (10.17) | 3/1 | 11.00 | 3.57 |
| k_{bca}^+ | 5477 | $K_{ad} = K_{da}$ | 10.57 (10.22) | 6/1 | 11.35 | 3.74 |
| | | $K_{bc} = K_{cb}$ | 9.96 (9.61) | | | |
| | | $K_{ac} = K_{ab}$ | 10.59 (10.24) | | | |
| | | $K_{ab} = K_{dc}$ | 9.46 (9.11) | | | |
| | | $K_a = K_d$ | 10.59 (10.22) | | | |
| | | $K_b = K_c$ | 10.66 (10.29) | | | |

^a Macroscopic, k , and microscopic, k , rate constants determined as described in the text. The subscripts indicate the basic nitrogens, and the last letter indicates the nucleophilic one. ^b Macroscopic acidity constants, K , in this work were determined by pseudo-titration (see Materials and Methods). Values in parentheses are the ones estimated by Aikens et al.²⁴ using methods introduced by Smith and Martell.²⁵ The first entry in the parentheses is the one calculated from the microscopic value, and the second entry is the one from the measured value. Microscopic constants in this work (values outside parentheses) were determined by extrapolation of the calculated values in parentheses. For the notation for microscopic acidity constants, K , see Figure 5. ^c Statistical corrections: p = number of ionizable protons, q = number of basic sites. ^d Determined via thermodynamic cycles using Figure 5.

pH 9.27 and 0.144 at pH 9.81 which indicates the increasing importance of the k_3 pathway. Values for $k_2 = 640 \pm 150 M^{-1} h^{-1}$ and $k_3 = 2550 \pm 500 M^{-1} h^{-1}$ were determined from a second-order curve fit such that the x term is defined as $k_2 K_2$ and the x^2 term as $k_3 K_2 K_3$ (eq 23 and Figure 2). Analysis using eq 23 provides an intercept equal to $k_1 = 108 \pm 40 M^{-1} h^{-1}$ that is considered less accurate than the $k_1 = 150 \pm 30 M^{-1} h^{-1}$ obtained from the slope of a plot of the left-hand parameter of eq 24 as a function of $[H^+]$. The data do not allow for the determination of the rate constant k_4 , because $[spm^0]$ is negligible even at the highest pH used. The macroscopic rate constants for spm are included in Table 4.

Product Distribution [PA-pG]/[5'GMP]. An alternative way of analysis looks at the observed product ratios between 5'GMP and PA. This ratio can only be obtained in the neutral and slightly acidic region where hydrolysis competes effectively with the nucleophilic substitution by the polyamine, so that this analysis is limited to the pH range $pH \leq 8.63$. According to eq 15, the product ratio is given by eq 25:

$$\frac{[spd-pG]}{[5'GMP]} = \frac{k_1[H_2spd^{2+}] + k_2[Hspd^+] + k_3[spd^0]}{k_{SH}^w + k_{SH}^{OH}[OH^-]} \quad (25)$$

A plot of $[spd-pG]/[5'GMP]$ vs $[spd]_{tot}$ has a slope, S_p , given by eq 26. $spd-pG$ stands for both isomers. S_p values are included in Table 1. It is easily seen by comparing eqs 17 and 26 that $S_p = S_k/I$ where I represents the contribution to the rate by the hydrolysis

and is given by $I = [H^+](k_{SH}^w + k_{SH}^{OH}[OH^-])/(K_a^{SH} + [H^+])$. Table 1 indicates that the agreement between S_p and S_k/I is fairly good. However, there appears to be a trend toward increasing disagreement with increasing pH, most likely because the observed product ratios become very large and therefore less accurate.

$$S_p = \frac{k_1/F_{spd} + k_2 K_2/[H^+]F_{spd} + k_3 K_2 K_3/[H^+]^2 F_{spd}}{k_{SH}^w + k_{SH}^{OH}[OH^-]} \quad (26)$$

Similarly, S_p obtained from the slope of a plot of $[spm-pG]/[5'GMP]$ vs $[spm]_{tot}$ exhibits a good agreement with the S_k/I values (see Table 1), indicating self-consistency of the analysis.

Assignment of spd_a-pG and spd_c-pG . Several lines of evidence, discussed earlier, indicated that the two observed product peaks had to be assigned to products derived from reactions by primary amino groups. Isomer spd_a-pG was assigned to the first and spd_c-pG to the second eluting compound (see structures and Figure 3) on the basis of the reasoning presented below. The ratio of the two peaks, $[spd_a-pG]/[spd_c-pG]$, varied smoothly between the lowest and highest pH, namely from 2.40 at pH 6.1 to 0.71 at pH 11.87 (Table 2). The observation of the small but significant variation of the isomeric ratio as a function of pH is consistent only with the model of microscopic ionization postulated by Onasch and co-workers^{22a} and not with other models that presume either a large difference or identical values for the microscopic pK_s of N_a and N_c (more on this in the Discussion). Therefore, we analyzed our results on the basis of the constants reported by Onasch,^{22a} and the assignment of the peaks in Figure 3 was done as follows: At $pH \approx 11.9$, most of spd is present as spd^0 , and therefore, the relative abundance of N_a vs N_c approaches unity. Under these conditions, the most basic N should also be the most nucleophilic and favor the corresponding product. Since, according to Onasch's work N_c is more basic than N_a , the largest peak in the high-pH experiments should be assigned to the spd_c-pG which is the second appearing under our chromatography conditions. In the low pH range, the relative abundance favors the amino group with the lowest pK , i.e. $[H_2spd_a^{2+}] > [H_2spd_c^{2+}]$, and this results in the preponderance of the spd_a-pG product. After obtaining both the microscopic acidity constants and rate constants (see below), a computer simulation was able to reproduce the observed product ratios within $\pm 5\%$ over the entire pH range.²³

Estimation of the Microscopic Ionization Constants for spd and spm . Because of the negligible

(22) (a) Onasch, F.; Aikens, D.; Bunce, S.; Schwartz, H.; Nairn, D.; Hurwitz, C. *Biophys. Chem.* **1984**, *19*, 245. (b) Onasch and co-workers^{22a} reported both macroscopic and microscopic acidity constants for spd determined using two-dimensional heteronuclear-coupled NMR monitoring ^{13}C and 1H chemical shifts. They were able to confirm the macroscopic values obtained from NMR by titration. Onasch's values were determined at 20 °C with 0.1 M spd (ionic strength between 0.3 and 0.6 M, no compensating electrolyte), whereas ours were done at 23 °C and 1 M ionic strength. The change in ionic strength is most likely responsible for the difference in the pK_a s between our study and theirs. This assertion is supported by the observation that macroscopic pK_a values as determined here and by Onasch agree better as the charge density of the polyamine decreases, with near perfect agreement observed for K_3 .

(23) Baird, E. E. Chemistry Senior Thesis, University of California, Santa Cruz, CA, 1993. (a) Computer simulations of the product ratios were performed using Microsoft Excel on a Mac IICI. (b) Relative abundances of all microstates presented in Figure 4 for spd and Figure 5 for spm as a function of pH are determined using a partition function approach.

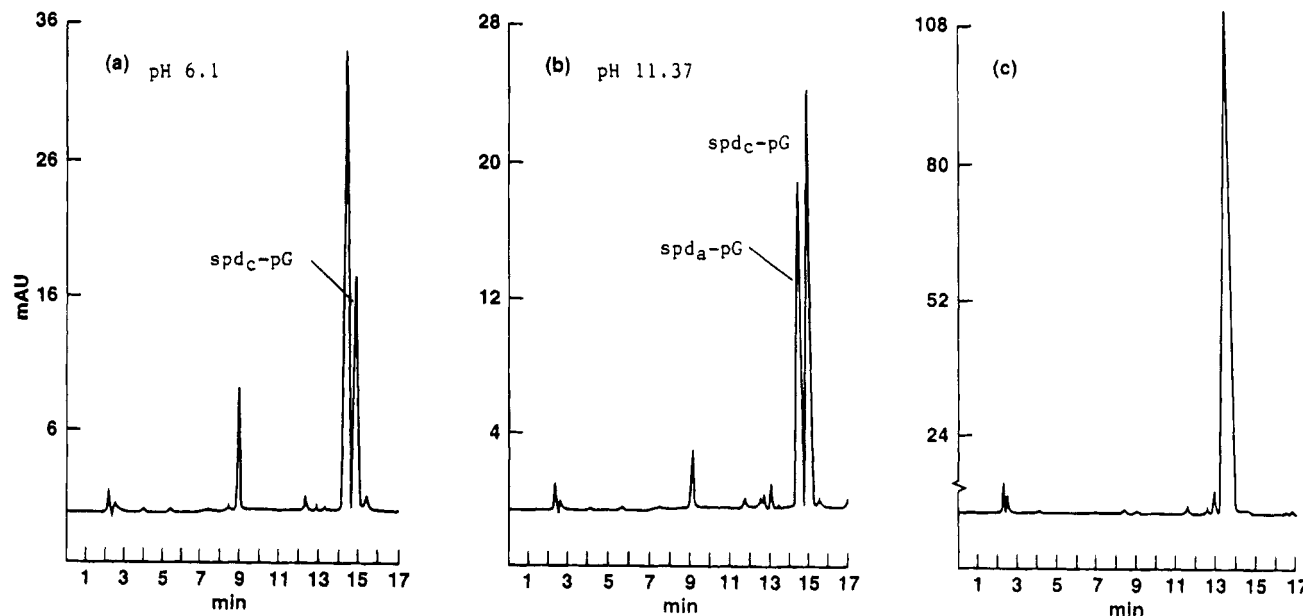


Figure 3. HPLC profiles of resolved spd-pG isomers from reaction mixture of 0.05 M spd with 0.0005 M 2-MeImpG at 37 °C. (a) pH 6.1. (b) pH 11.37. (c) HPLC profile of reaction mixture of 0.05 M 3,3-spd (symmetrical) with 0.001 M 2-MeImpG at pH 9.03 and 37 °C.

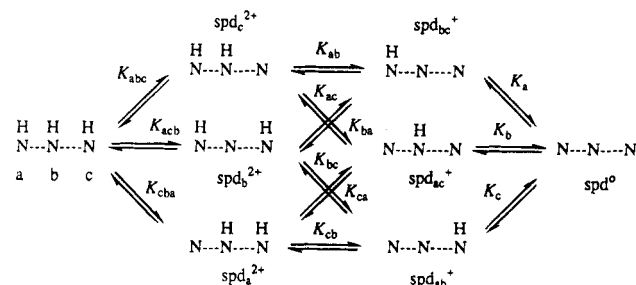


Figure 4. Microscopic ionization equilibria of spermidine. Species are labeled with subscripts to identify the deprotonated site(s). The microscopic acidity constants, K , are labeled with subscripts that identify the protonated positions, with the last letter in the subscript denoting the position that loses the proton.

reactivity of the secondary amino groups of the PAs under our conditions, it may be inappropriate to correlate the macroscopic rate constants with the corresponding macroscopic ionization constants. A more meaningful correlation could be attained by relating the microscopic rate constants with the corresponding microscopic acidity constants. To the best of our knowledge, this is the first time such an attempt is being made. To do that, it was necessary to estimate the microscopic ionization constants as well as the microscopic rate constants for our system. All possible ionization equilibria of spd and spm are illustrated in Figures 4 and 5, respectively. Species are labeled with subscripts to identify the deprotonated site(s). The microscopic acidity constants, K , are labeled with subscripts that identify the protonated positions, with the last letter in the subscript denoting the position that loses the proton. K values under our conditions were estimated from the appropriate constants determined by Onasch^{22a} for spd and by Aikens²⁴ for spm in the spirit of eq 27.¹⁷ In eq 27, the determination of K_{abc} of spd is shown as a specific example. The difference between our macroscopic values and theirs was attributed to the

$$K_{abc}(\text{ours}) = K_{abc}(\text{Onasch}) \times \frac{K_1(\text{ours})}{K_1(\text{Onasch})} = K_{abc}(\text{Onasch})/2.34 \quad (27)$$

different ionic strength of the medium.^{22b,24} In extrapolating from their constants, we assumed that the effect of the ionic strength on the macroscopic pKs is the same as the effect on the microscopic values and identical for primary and secondary amino groups.

All macro- and microscopic acidity constants, including the ones reported by Onasch and Aikens, are listed in Tables 3 (spd) and 4 (spm). It is interesting to compare the relative basicities of the three amino groups in spd.^{22a} At low pH where there is a high degree of overall protonation, the most acidic is the secondary amino group, $pK_{acb} < pK_{abc}, pK_{cba}$, because of the base-weakening effect of the two neighboring protonated amino groups, N_a and N_c . Furthermore, $pK_{abc} > pK_{cba}$ because the distance of the N_c group from the neighboring protonated N_b group is larger ($(\text{CH}_2)_4$) than the distance of the N_a group ($(\text{CH}_2)_3$) from the N_b group. The same order, $pK_c > pK_a$, is seen even in the high-pH range when the degree of protonation approaches zero. However, the higher intrinsic basicity of the secondary amino group, N_b , outweighs the diminished base-weakening effect of the deprotonated amino groups, so that pK_b is larger than pK_a and only slightly smaller than pK_c .

Determination of Microscopic Rate Constants for the Reaction of spd and spm with 2-MeImpG. Microscopic rate constants, k , were assigned subscripts to indicate the basic nitrogens, and the last letter in the subscript identifies the nucleophilic site. k values were estimated from the macroscopic ones by assuming that, within each family of nucleophiles, e.g. diprotonated, a Bronsted-type structure reactivity relationship applies. The Bronsted slope (β_{nuc}) was set equal to 0.48 which was obtained in the reaction of 2-MeImpG with primary monoamines.¹⁴ When appropriate, statistically corrected parameters were included in the calculations. A detailed analysis is presented elsewhere.¹⁷ The obtained microscopic rate constants, as well as the statistical corrections are included in Tables 3 (spd) and 4 (spm). The analysis

(24) Aikens, D.; Bunce, S.; Onasch, F.; Parker, R., III; Hurwitz, C.; Clemans, S. *Biophys. Chem.* **1983**, *17*, 67.

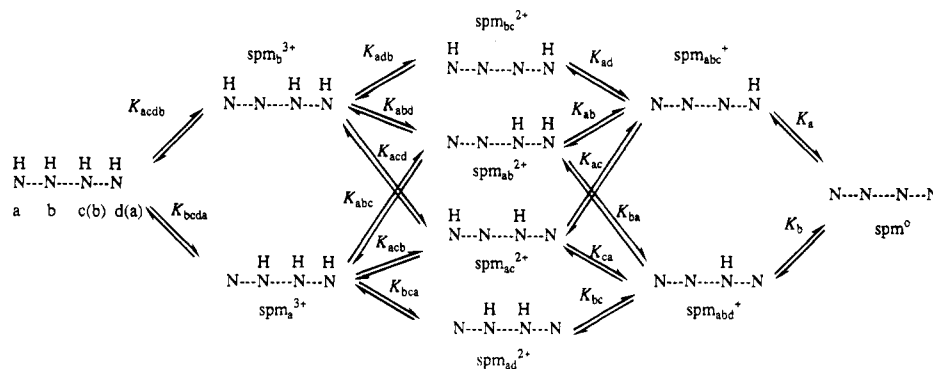


Figure 5. Microscopic ionization equilibria of spermine. Species are labeled with subscripts to identify the deprotonated site(s). The microscopic acidity constants, K , are labeled with subscripts that identify the protonated positions, with the last letter in the subscript denoting the position that loses the proton. Because of the symmetry of the molecule, the subscripts of the protonation constants can be defined in two ways (only one given here, both notations given in Table 4).

is summarized below. Equations 28 and 29 were used for the spd and eqs 30–32 for the spm data. The relative concentrations of the various species are expressed as a function of the appropriate micro- and macroscopic acidity constants. For example, $[\text{spd}_a^{2+}]/[\text{spd}^{2+}]_{\text{tot}} = K_{\text{cba}}/K_1$ where spd_a^{2+} refers to $\text{H}_2\text{spd}_a^{2+}$ and spd^{2+} refers to $\text{H}_2\text{-spd}^{2+}$; for simplicity, we shall henceforth drop the hydrogens. Equation 28 relates the macroscopic rate constant k_1 to the microscopic rate constants where k_a^{2+} and k_c^{2+} are the microscopic rate constants for the reaction by the spd_a^{2+} and spd_c^{2+} species, respectively (see Figure 4). Since one constant can be expressed as a function of the other via the Brønsted relationship we find $k_c^{2+} = 686 \text{ M}^{-1}\text{h}^{-1}$ and $k_a^{2+} = 353 \text{ M}^{-1}\text{h}^{-1}$.

$$k_1[\text{spd}^{2+}]_{\text{tot}} = k_a^{2+}[\text{spd}_a^{2+}] + k_c^{2+}[\text{spd}_c^{2+}] \quad (28)$$

The relationship between k_2 and the corresponding microscopic rate constants is given by eq 29. In eq 29, k_{bc}^+ is the rate constant for attack by N_c of the spd_{bc}^+ species, k_{ba}^+ is the rate constant for attack by N_a of the spd_{ab}^+ species, and k_{ac}^+ and k_{ca}^+ are the rate constants for attack by N_c and N_a , respectively, of the spd_{ac}^+ (see Figure 4). From eq 29, we obtained $k_{\text{ca}}^+ = 775 \text{ M}^{-1} \text{ h}^{-1}$, $k_{\text{ba}}^+ = 1814 \text{ M}^{-1} \text{ h}^{-1}$, $k_{\text{bc}}^+ = 2240 \text{ M}^{-1} \text{ h}^{-1}$, and $k_{\text{ac}}^+ = 1504 \text{ M}^{-1} \text{ h}^{-1}$.

$$k_2[\text{spd}^+]_{\text{tot}} = k_{\text{ba}}^+[\text{spd}_{\text{ab}}^+] + k_{\text{bc}}^+[\text{spd}_{\text{bc}}^+] + (k_{\text{ac}}^+ + k_{\text{ca}}^+)[\text{spd}_{\text{ac}}^+] \quad (29)$$

The equilibria for the ionization of spm are presented in Figure 5. Due to the symmetry of the molecule, the notation for most equilibrium constants can be given in two ways. The equivalent acidity constants are included in Table 4, but for clarity, only one notation is included in Figure 5. Microscopic acidity constants were determined on the basis of values reported by Aikens et al.²⁴ by extrapolating to our ionic conditions in the spirit described by eq 27. It should be mentioned that, in contrast to spd, the microscopic acidity constants for spm are estimated²⁵ and not experimentally determined. Equation 30 relates the macroscopic rate constant k_1 to

the microscopic rate constant k_a^{3+} for reaction by the spm_a^{3+} species. From there, one obtains $k_a^{3+} = 1537 \text{ M}^{-1} \text{ h}^{-1}$.

$$k_1[\text{spm}^{3+}]_{\text{tot}} = k_a^{3+}[\text{spm}_a^{3+}] \quad \text{which after substitution gives}$$

$$k_a^{3+} = k_1 \frac{K_1}{K_{\text{bcda}}} \quad (30)$$

The k_2 process is described by eq 31 as the sum of the following processes: (i) reaction of N_a (N_d) of $\text{spm}_{\text{ab}}^{2+}$ with a rate constant of k_{ba}^{2+} , (ii) reaction of N_a of $\text{spm}_{\text{ac}}^{2+}$ with a rate constant of k_{ca}^{2+} , and (iii) reaction of N_a of $\text{spm}_{\text{ad}}^{2+}$ with a rate constant of $k_{\text{da}}^{2+} = k_{\text{ad}}^{2+}$. After appropriate manipulations of eq 31, we find $k_{\text{ad}}^{2+} = 1684 \text{ M}^{-1} \text{ h}^{-1}$, $k_{\text{ba}}^{2+} = 4320 \text{ M}^{-1} \text{ h}^{-1}$, and $k_{\text{ca}}^{2+} = 1239 \text{ M}^{-1} \text{ h}^{-1}$. Finally,

$$k_2[\text{spm}^{2+}]_{\text{tot}} = k_{\text{ba}}^{2+}[\text{spm}_{\text{ab}}^{2+}] + k_{\text{ca}}^{2+}[\text{spm}_{\text{ac}}^{2+}] + k_{\text{ad}}^{2+}[\text{spm}_{\text{ad}}^{2+}] \quad (31)$$

the k_3 process is expressed by eq 32 which includes the reactivity of N_a of the $\text{spm}_{\text{abc}}^+$ with a rate constant designated k_{bca}^+ and the reactivity of $\text{spm}_{\text{abd}}^+$ with rate constants designated k_{abd}^+ for reaction by N_d and k_{dba}^+ for reaction by N_a . We find $k_{\text{abd}}^+ = 1067 \text{ M}^{-1} \text{ h}^{-1}$, $k_{\text{bca}}^+ = 5477 \text{ M}^{-1} \text{ h}^{-1}$, and $k_{\text{dba}}^+ = 3724 \text{ M}^{-1} \text{ h}^{-1}$.

$$k_3[\text{spm}^+]_{\text{tot}} = k_{\text{bca}}^+[\text{spm}_{\text{abc}}^+] + (k_{\text{abd}}^+ + k_{\text{dba}}^+)[\text{spm}_{\text{abd}}^+] \quad (32)$$

Discussion

Bronsted Plot of the Reaction of the Primary Amino Groups in spm and spd with 2-MeImpG. All the microscopic rate constants obtained for the reaction of 2-MeImpG with spm and spd are plotted together in Figure 6 as a function of the corresponding microscopic pK (both rate and acidity constants statistically corrected). There are a total of 13 bases spanning 2 pK units; they comprise five different families, i.e. the K_1 -(spd) with two points deviating negatively from the dashed line, the K_2 -(spd) with four points that define the dashed line, the K_1 -(spm) with one point lying somewhat lower than the solid line, and finally the K_2 -(spm) and K_3 -(spm) which nicely lie on the solid line. For comparison, we included in Figure 6 the corresponding point, filled square, for the reaction of *n*-butylamine with

(25) Smith, R. M.; Martell, A. E. *Critical stability constants*; Plenum Press: New York, 1975; Vol. 2

(26) Kimberley, M. M.; Goldstein, J. H. *Anal. Chem.* **1981**, *53*, 789.

(27) Hague, D. N.; Moreton, A. D. *J. Chem. Soc., Perkin Trans. 2* **1994**, 265.

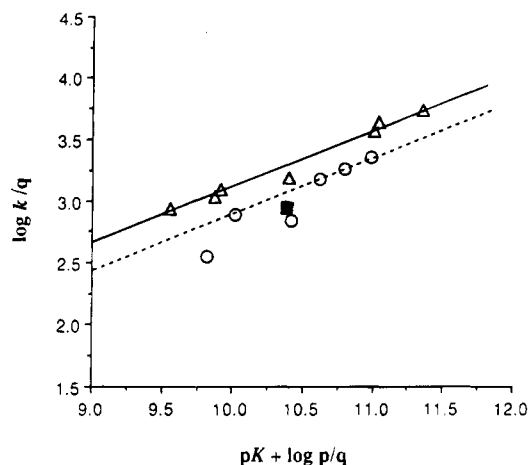


Figure 6. Bronsted plot of microscopic rate constants vs Bronsted acidity constants (p and q refer to statistical corrections, see the text and Tables 3 and 4) in the reaction of spermidine (circles) and spermine (triangles) with 2-MeImpG at 37 °C in water, $\mu = 1.0$ M with NaCl. Both lines drawn with a slope of 0.48. The filled square represents the corresponding reaction with *n*-butylamine (ref 14).

2-MeImpG.¹⁴ The fact that each family defines a line with a slope of about 0.48 is not surprising since the rate constants within each family are interrelated via Bronsted-type relationships with a $\beta_{\text{nuc}} = 0.48$ (see microscopic rate constants determinations). On the other hand, the fit of all three spm families on one plot (solid line) was not necessarily predictable considering that the corresponding pK s are estimated.^{24,25} The good fit of the spm data on one single line shows that triply, doubly, or singly protonated species exhibit comparable intrinsic reactivity at least under our conditions. Therefore, the less than perfect match of the two spd families cannot be attributed to the different charge between spd^{2+} and spd^+ . The negative deviation of the $K_1(\text{spd})$ family is too large to be attributable to experimental uncertainty in determining the rate constant k_1 ; one possible explanation is that, perhaps, the corresponding microscopic acidity constants, K_{cba} and K_{abc} , are underestimated. By and large, the reactivity of the primary amino groups in spm and spd is not strikingly different from that of a typical primary amine in the reaction with 2-MeImpG, a conclusion that may or may not have been predictable.

Degree of Protonation of spd over the Range 6.1 \leq pH \leq 11.9. Establishing a structure–reactivity relationship for the two polyamines, as described above, shows the feasibility of such an exercise and brings a strong level of confidence to the microscopic acidity constants we used. Furthermore, the determination of the ratio of the two spd-pG isomers over a large pH range (Table 2) bears directly on the relative degree of protonation of the two primary amino groups of spd. The observed ratio is inconsistent with the suggestion by Takeda and co-workers that the degree of protonation for monoprotonated spd is 0.0, 0.0, and 1.0 and for diprotonated spd is 1.0, 0.0, and 1.0 for N_a , N_b , and N_c , respectively.²⁸ Takeda's conclusions²⁸ would have predicted the observation of only one isomer, i.e. $\text{spd}_c\text{-pG}$, at high pH and the observation of an increasing amount of $\text{spd}_a\text{-pG}$ with decreasing pH, reaching a ratio equal to 1 at neutral pH. Similarly, our results are inconsistent

with the proposal by Delfini and co-workers that the degree of protonation for monoprotonated spd is 0.5, 0.0, and 0.5 and for diprotonated spd is 1.0, 0.0, and 1.0 for N_a , N_b , and N_c , respectively.²⁹ Delfini's proposal²⁹ would have predicted a product ratio that is equal to 1 in the whole pH range. The observation that the product ratio varies with pH, but that it is not drastically different from unity is consistent, as mentioned earlier, with the conclusion^{22a,26,27} that at each point in the protonation sequence all basic sites are protonated to a significant degree. This implies that all basic sites could exhibit nucleophilicity to a significant degree unless another effect, such as steric hindrance, counteracts it.

Stability/Reactivity of 2-MeImpG in the Presence of Polyamines. Since one of the objectives of undertaking this work was to use the polyamines as facilitators in non-enzymatic template-directed polynucleotide synthesis reactions, an experiment was performed at pH 7 (0.25M HEPES) at 7 °C in the presence of 0.1 M Mg^{2+} and 1 M ionic strength. It is found that, after 14 days of incubation at 7 °C, no more than 12% of the 2-MeImpG starting material is consumed by spm. This incubation time is representative of the time scale of polymerization reactions, and hence, our result shows that depletion of 2-MeImpG by reaction with spm is not a major concern.

A more detailed picture of the stability of 2-MeImpG as a function of pH and amine concentration in the presence of spd or spm is gained by inspection of Tables S2 and S3 (in the supporting information),¹⁷ respectively. We are comparing the reaction of PA with hydrolysis. The comparison can be accomplished by looking for the conditions that produce a product ratio, $[\text{PA-pG}]/[5'\text{GMP}]$, approximately equal to 1. For example, at pH 6.20, a concentration of 0.05 M spd is required to produce $[\text{spd-pG}]/[5'\text{GMP}] = 1.07$. At pH 6.99, 0.01 M spd produces a ratio of 0.75 and at pH 7.50 a ratio of 1.94 (Table S2 in the supporting information).¹⁷ Similarly, in the reaction with spm, at pH 6.16, 0.05 M spm produces $[\text{spm-pG}]/[5'\text{GMP}] = 0.78$, at pH 6.92, 0.01 M amine produces a ratio of 0.94, and at pH 7.7, 0.003 M a ratio of 0.95 (Table S3 in the supporting information).¹⁷ In general, one can use eq 33 and our data in Table 1 in order to estimate conditions under which the nucleophilicity of the corresponding amine will be low enough to be acceptable.³¹ For example, from eq 33, we find that, for a product ratio of about 1 at pH 7.99, a spd concentration of 0.0016 M is required and that, at pH 8.12, a spm concentration of 0.00097 M is required.

$$\frac{[\text{PA-pG}]}{[5'\text{GMP}]} = \frac{S_k}{I} [\text{PA}]_{\text{tot}} \quad (33)$$

(29) Delfini, M.; Segre, A. L.; Conti, F.; Barbucci, R.; Barone, V.; Ferruti, P. *J. Chem. Soc., Perkin Trans. 2* **1980**, 900.

(30) Reference for $K_w \approx 2 \times 10^{-14} \text{ M}^{-2}$ at 27 °C, $[\text{NaCl}] = 1 \text{ M}$: Harned, H. S.; Owen, B. B. *The Physical Chemistry of Electrolytic Solutions*; Reinhold: New York, 1950; p 488. Our values were $K_w = 2.1 \times 10^{-14} \text{ M}^{-2}$ at 37 °C, $[\text{NaCl}] = 1 \text{ M}$.^{19b}

(31) It should be noted that eq 33 refers to conditions where the nucleotide is the minor component (pseudo-first-order). The nucleophilicity may be somewhat altered, if $[\text{PA}] \approx [2\text{-MeImpG}]$ because an additional product, the disubstituted one, is formed. With respect to the reactivity of spm and spd toward nucleotides other than 2-MeImpG, we have reasons to believe that the reactivity pattern will be similar. Our belief is based on a hydrolysis profile of ImpG which is very similar to the one of 2-MeImpG in the range $7.5 \leq \text{pH} \leq 9.5$ ^{19b} and on experiments with other nucleobases which indicate that the base does not greatly affect the reactivity of the substrate toward various nucleophiles.^{16b,20}

(28) Takeda, Y.; Samejima, K.; Nagano, K.; Watanabe, M. Sugeta, H.; Kyogoku, Y. *Eur. J. Biochem.* **1983**, *130*, 383.

PAs vs Polyammonium Macrocycles: Similarities and Differences. The nonreactivity of the secondary amino groups of spd and spm is in striking contrast with the observed reactivity of secondary amino groups in polyammonium macrocycles, such as $[24]N_6O_2$.⁶⁻¹¹ Evidence has been accumulated for the formation of an intermediate phosphate-macrocycle, with the phosphate from ATP^{8,9} or from acetylphosphate.¹⁰ The half-life for dephosphorylation of ATP at 70 °C⁹ and acetylphosphate at 40 °C¹⁰ in the presence of $[24]N_6O_2$ at pH 7 is approximately 10 min; this is to be compared with an upper estimate of about 1 month for nucleotidyl transfer from ImpN to the secondary amino group in 0.04 M spm at 37 °C (based on this work and ref 14). An additional difference between the two seemingly similar systems, i.e. polyamines with ImpNs and polyammonium macrocycles with the triphosphates of the nucleosides, is that the former exhibits no detectable complex formation of the reactants. We have attributed the slight downward curvature of the buffer plots to amine-ammonium rather than ImpN-ammonium association. On the other hand, the complex between ATP and $[24]N_6O_2$ is proposed to be quite stable, as indicated by ³¹P NMR.⁹ One explanation we can offer for these differences is that the multiply negatively charged triphosphates offer three point charges for electrostatic attraction with the multiply charged polyammonium macrocycles to stabilize complex formation. In contrast, interaction of polyamines with ImpNs that either are zwitterionic or carry one negative charge must be minimal. In addition, the three electrostatic interactions between ATP and the macrocycles are proposed to create a complex with a rigid, boatlike, configuration.⁹ It is plausible that within the boatlike structure a deprotonated ammonio group is forced to attain the configuration present in morpholine or piperidine rather than the acyclic PAs, and thus, the reactivity of the polyammonium macrocycle is more in tune with the reactivity of those alicyclic amines and not PAs (the secondary amino groups in morpholine and piperidine are reactive toward ImpNs¹⁴).

Conclusions

The work described here establishes the kinetics of the reaction of spd and spm with 2-MeImpG in water at 37 °C in the range 6 < pH < 11 and with an ionic strength of 1.0 M maintained with NaCl. Interestingly, only the primary amino groups are reactive, whereas the secondary amino groups are at least 100 times less reactive, most likely because of a steric effect. In contrast to the

negligible reactivity of the secondary amino group of spd and spm observed in our study, derivatives thereof, i.e. the polyammonium macrocycles studied and used extensively as ATPase mimics, show enhanced reactivity with the triphosphates of the nucleosides. In other words, the secondary amino groups of the macrocycles are quite reactive toward ATP which is much less reactive than the phosphoimidazolidine derivatives of the nucleosides, such as 2-MeImpG. Possible reasons for this disparity are discussed.

Analysis of the kinetic data in conjunction with an estimate of the microscopic acidity constants, *K*, and an estimate of the relative reactivity of the primary amino groups allows most of the microscopic rate constants, *k*, to be estimated. A Bronsted plot for spm (see Figure 6) exhibits an excellent correlation between the microscopic rate constant and the corresponding p*K*s and a less satisfactory correlation for spd. It is concluded that the primary amino group of the natural polyamines, spd and spm, behave very similarly as aliphatic primary amines of comparable basicity.

The distribution of the two isomeric spd-pG products which was obtained for the range 6 < pH < 11 is consistent with the idea of microscopic acidity constants for the polyamines and inconsistent with stepwise protonation. The isomeric distribution of the two spd-pG products agrees well with the relative degree of protonation proposed for spd by Onasch et al.,^{22a} Kimberley and Goldstein,²⁶ and Hague and Moreton²⁷ but is inconsistent with the conclusions of Takeda et al.²⁸ and Delfini et al.²⁹

Acknowledgment. This research was supported by Grant No. NCC 2-534 from the Exobiology Program of the National Aeronautics and Space Administration. We thank Dr. S. Chang from the Planetary Biology Branch of the NASA/Ames Research Center and Prof. C. F. Bernasconi from the Chemistry Department of the University of California at Santa Cruz for providing the facilities and for discussions.

Supporting Information Available: Kinetic and product distribution Data (Tables S1–S3), distribution profile of spermine species as a function of pH calculated on the basis of the determined acidity constants (Figure S1), and calculation of microscopic acidity and microscopic rate constants (11 pages). This material is contained in libraries on microfiche, immediately follows this article in the microfilm version of the journal, and can be ordered from the ACS; see any current masthead page for ordering information.

JO941686E